

# ShapeSpeak: Body Shape-Aware Textual Alignment for Visible-Infrared Person Re-Identification

Shuanglin Yan<sup>1</sup>, Neng Dong<sup>1</sup>, Shuang Li<sup>2</sup>, Rui Yan<sup>1</sup>, Hao Tang<sup>3</sup>, Jing Qin<sup>3</sup>

<sup>1</sup>Nanjing University of Science and Technology

<sup>2</sup>Chongqing University of Posts and Telecommunications

<sup>3</sup>The Hong Kong Polytechnic University

## ABSTRACT

Visible-Infrared Person Re-identification (VIReID) aims to match visible and infrared pedestrian images, but the modality differences and the complexity of identity features make it challenging. Existing methods rely solely on identity label supervision, which makes it difficult to fully extract high-level semantic information. Recently, vision-language pre-trained models have been introduced to VIReID, enhancing semantic information modeling by generating textual descriptions. However, such methods do not explicitly model body shape features, which are crucial for cross-modal matching. To address this, we propose an effective Body Shape-aware Textual Alignment (**BSaTa**) framework that explicitly models and utilizes body shape information to improve VIReID performance. Specifically, we design a Body Shape Textual Alignment (BSTA) module that extracts body shape information using a human parsing model and converts it into structured text representations via CLIP. We also design a Text-Visual Consistency Regularizer (TVCR) to ensure alignment between body shape textual representations and visual body shape features. Furthermore, we introduce a Shape-aware Representation Learning (SRL) mechanism that combines Multi-text Supervision and Distribution Consistency Constraints to guide the visual encoder to learn modality-invariant and discriminative identity features, thus enhancing modality invariance. Experimental results demonstrate that our method achieves superior performance on the SYSU-MM01 and RegDB datasets, validating its effectiveness.

## KEYWORDS

Visible-infrared person re-identification, body shape textual alignment, text-visual consistency, distribution consistency

## 1 INTRODUCTION

Person re-identification (ReID) aims to retrieve images of the same individual across different, non-overlapping cameras. While visible-spectrum ReID [18, 23, 47, 61] has made remarkable progress, it still struggles under low-light or nighttime conditions due to the inability of visible cameras to capture discriminative features. To address this, visible-infrared person re-identification (VIReID) [68] has emerged. Infrared cameras can capture person appearance regardless of lighting conditions, enhancing the applicability of ReID. However, the main challenge of VIReID lies in the substantial modality gap between infrared and visible images, which complicates cross-modal feature alignment and identity matching, presenting a major obstacle to cross-modal ReID systems.

To reduce the significant modality gap caused by heterogeneous data sources, existing methods are broadly categorized into generative and non-generative approaches. Generative methods [33, 35, 44], especially those based on generative adversarial networks

(GANs) [12], attempt to synthesize cross-modal images or intermediate domain representations to facilitate learning. These methods provide direct pixel-level supervision, reducing the domain gap at the image level. However, generated images often contain artifacts and inconsistencies, which can mislead the model. Additionally, the instability of generative training and the need for careful tuning make these approaches challenging to scale and deploy in real-world scenarios. In contrast, non-generative methods [39, 41, 65] focus on learning a shared feature space for directly aligning infrared and visible representations. This is typically achieved through network design, metric learning strategies, or contrastive objectives that enforce cross-modal similarity. Although these methods avoid the instability of image synthesis, their exclusive reliance on identity-level supervision constrains the model's capacity to capture high-level semantics, making it challenging to maintain both modality-invariant and identity-discriminative features simultaneously.

In recent years, vision-language pretraining (VLP) models have rapidly advanced, leveraging language supervision to train visual encoders with exceptional high-level semantic extraction capabilities. Inspired by this, study [66] was the first to introduce the VLP model CLIP [37] to address the aforementioned challenges. This approach generates separate textual descriptions for visible and infrared images, and integrates their textual representations to guide the visual network in learning identity-related high-level semantic information. Specifically, it employs a vision-language alignment mechanism to introduce semantic supervision in VIReID, mitigating modality mismatches caused by significant differences in appearance, lighting conditions, and texture between infrared and visible images. The core assumption is that textual descriptions can provide additional high-level semantic information, such as body shape and clothing categories, thereby compensating for the modality misalignment that may arise when relying solely on image-level features. However, this method still has notable limitations. While the method attempts to learn body shape information through textual descriptions, it does not explicitly model body shape features, instead relying on the model to automatically extract such information during contrastive learning. Since body shape is inherently modality-invariant and critical for VIReID, relying solely on implicit learning may hinder the model's ability to fully capture and leverage body shape features, ultimately limiting recognition performance.

Building upon this, we propose an effective Body Shape-aware Textual Alignment (**BSaTa**) framework to explicitly extract and utilize body shape information for enhancing feature representation in VIReID. The framework consists of two main components: a Body Shape Textual Alignment (BSTA) module and a Shape-aware

Representation Learning (SARL) module. The BSTA module uses an advanced human parsing model to analyze both visible and infrared images, extracting key body shape cues (such as body contours, limb proportions, and torso structure) to generate body shape maps, which are then encoded into visual shape features. These features are transformed into structured textual shape representations using CLIP's vision-language alignment capabilities. To ensure high-quality textual shape representations, we introduce a Text-Visual Consistency Regularizer (TVCR) that enforces symmetric alignment between the visual and textual shape features in a shared embedding space, enabling the textual shape representations to more accurately describe identity-related shape characteristics. The SARL module incorporates a multi-text supervision mechanism, which not only effectively guides the visual encoder to learn discriminative shape features but also enables the fully extraction of modality-invariant identity information. Furthermore, we design a distribution consistency constraint (DCC) that treats the identity-level text representation as an alignment anchor to reduce the distribution gap between visible and infrared modalities, thus enhancing cross-modal alignment. Compared to existing methods, our method explicitly models body shape information, enabling more effective extraction of modality-shared features and significantly improving recognition accuracy and generalization in VIREID.

Here are the main contributions of our paper: (1) We propose a body shape-aware textual alignment framework that explicitly extracts and utilizes body shape information, enhancing the model's ability to capture modality-invariant features. (2) We design a body shape textual alignment module with a cross-modal consistency regularizer that transforms body shape maps into structured textual representations, ensuring the quality of the generated textual representations. (3) We introduce a shape-aware representation learning mechanism that combines multi-text supervision and distribution consistency constraints to emphasize body shape information and enhance feature representation. (4) Extensive experiments demonstrate that our method achieves superior performance on both SYSU-MM01 and RegDB, validating its effectiveness.

## 2 RELATED WORK

### 2.1 Visible-Infrared Person Re-Identification

Visible-infrared person re-identification (VIREID) faces significant challenges due to the inherent modality gap [25] between infrared and visible images, which arises from their fundamentally different imaging principles. Unlike visible images [6, 8, 70] that capture detailed textures and colors under natural lighting, infrared images represent thermal radiation, often lacking fine-grained appearance details [42, 57, 60]. This discrepancy leads to substantial feature misalignment, making cross-modal retrieval highly challenging. Over the years, various strategies have been proposed to bridge this gap, which can be broadly categorized into generative and non-generative approaches.

Generative methods [1, 27, 33, 35, 44] aims to bridge the modality gap by synthesizing cross-modal images or intermediate domain representations, often utilizing generative adversarial networks (GANs) [12] or variational frameworks. For instance, Wang et al. [44] introduced a pixel alignment module based on GANs that transforms real visible images into synthetic infrared-like images

to mitigate the cross-modal discrepancy. While these methods help reduce the modality gap, they are often plagued by issues such as semantic distortion, mode collapse, and training instability, which hinder their generalization to real-world scenarios. Non-generative methods [7, 11, 26, 39, 41, 65, 66] have emerged as the dominant solution for VIREID due to their stability and effectiveness. These approaches [22, 29] primarily focus on learning modality-invariant and discriminative features through network architecture design, metric learning strategies, or contrastive objectives that enforce cross-modal similarity. Recently, vision-language pre-trained (VLP) models, such as CLIP [37], have been incorporated into VIREID, providing richer semantic supervision by generating textual descriptions [66]. However, this method mainly emphasizes appearance attributes and overlook the importance of body shape modeling [48], which is equally crucial for cross-modal identity discrimination. This paper addresses this gap by explicitly encoding shape information using structured textual shape representations.

### 2.2 Vision-Language Pre-Training

The "pre-training and fine-tuning" paradigm has become a cornerstone in computer vision, enabling models to transfer knowledge from large-scale datasets to various downstream tasks. Previous prevailing practice is rooted in the supervised unimodal pre-training [9, 13] on ImageNet [5]. Initially, pre-training was predominantly conducted on single-modal datasets like ImageNet [5], where models such as ResNet [13] and Vision Transformer (ViT) [9] relied on category labels for supervised learning to acquire powerful visual representations. While effective, this approach was inherently limited by the need for extensive labeled data and its inability to capture cross-modal relationships. To address these limitations, vision-language pre-training (VLP) has emerged as a promising alternative, shifting the focus from purely visual learning to multimodal representation learning. VLP models aim to bridge the gap between vision and language by leveraging large-scale multimodal data. Early works [2, 19, 20, 30, 46] explored joint vision-language representations through masked modeling and image-text alignment tasks, demonstrating improved semantic understanding across modalities. However, these methods often relied on complex multimodal fusion architectures, which added computational overhead and limited generalization. More recently, contrastive learning [14, 37, 63] has gained traction as a scalable and effective alternative. By leveraging contrastive objectives to distinguish between positive and negative pairs, models can learn robust and transferable representations. A notable example is Contrastive Language-Image Pre-training (CLIP) [37], which has shown impressive adaptability across various downstream tasks [32, 49, 56, 58]. In this work, we leverage CLIP's powerful semantic understanding to enhance the extraction of identity-related high-level semantics, with the goal of bridging the modality gap in VIREID.

### 2.3 Prompt Learning

Prompt learning has emerged as a powerful paradigm for adapting large-scale pre-trained models to specific tasks with minimal modifications. Initially introduced in natural language processing (NLP) [16, 38], this approach enables models to conditionally interpret tasks by providing carefully designed prompts. While early methods relied on manually crafted templates, recent advancements

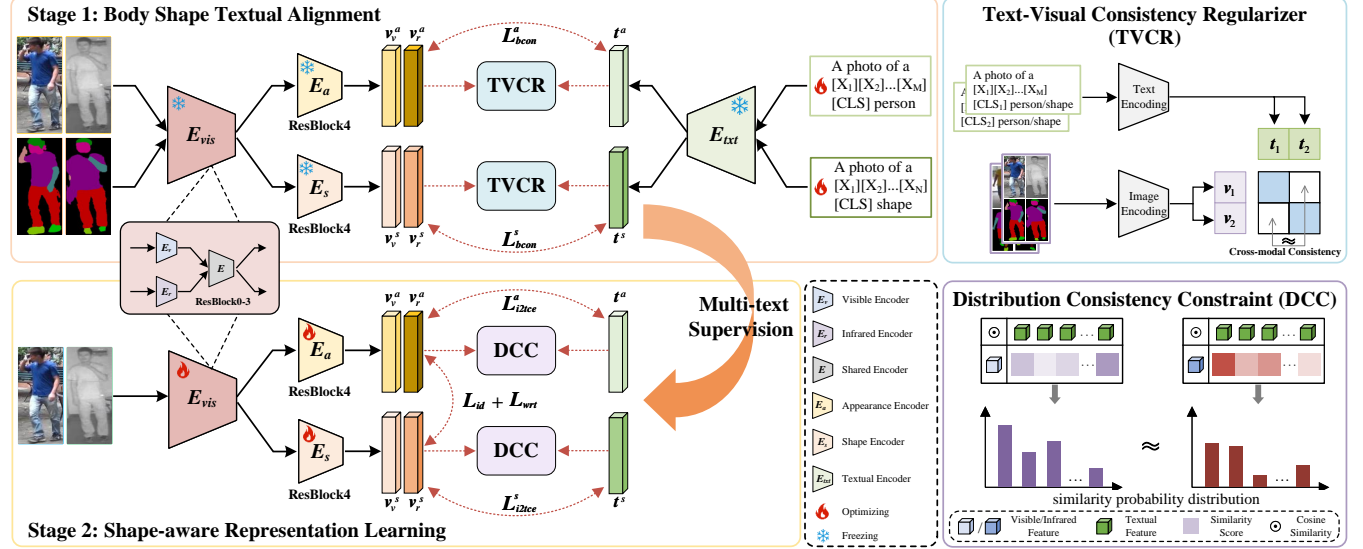


Figure 1: Overview of our BSaTa. It consists of two stages: Body Shape Textual Alignment (Stage 1) and Shape-aware Representation Learning (Stage 2). In Stage 1, we leverage the powerful cross-modal alignment capability of CLIP to generate identity-level textual shape and appearance representations for each infrared-visible image pair. A Text-Visual Consistency Regularizer (TVCR) is further introduced to ensure the semantic quality of the generated textual descriptions. In Stage 2, the textual representations generated in the previous stage are used as supervision to construct a Multi-text Supervision mechanism, which guides the training of the visual encoder. Additionally, a Distribution Consistency Constraint (DCC) is designed to utilize the textual features as anchors to enforce alignment between the feature distributions of infrared and visible modalities, thereby fully mining modality-invariant identity information and enhancing the feature representation capability. During inference, the shape and appearance features of both infrared and visible images are extracted, concatenated, and used for retrieval.

have shifted toward automated prompt optimization, mitigating issues such as instability and domain bias. In computer vision, prompt learning has gained traction, particularly in vision-language models. CoOp [73] pioneered learnable text prompts for adapting CLIP to various visual recognition tasks, eliminating the need for manual prompt engineering. CoCoOp [43] further advanced this concept by introducing conditional prompt tuning, which enhances generalization across unseen categories. These developments highlight the potential of prompt learning for leveraging vision-language representations in robust model adaptation. Despite these successes, applying prompt learning to fine-grained tasks [59], such as person re-identification, remains challenging. Recent work, such as CLIP-ReID [24], has attempted to bridge this gap by generating pedestrian descriptions for identity discrimination. Inspired by this, we propose leveraging prompt learning to generate modality-shared appearance and body shape descriptions for extracting high-level semantics in VIREID.

### 3 THE BSATA FRAMEWORK

Our proposed BSaTa is a conceptually simple yet effective framework, as shown in Figure 1. We begin by extracting visual features from both infrared and visible images using a visual backbone network. These features are then passed through the Body Shape Textual Alignment module, which generates structured textual shape representations. Finally, the generated textual shape representations serve as semantic guidance to supervise the backbone network,

enabling it to better capture modality-invariant body shape information and thereby enhancing the feature representation capability for VIREID.

#### 3.1 Feature Extraction

Given the sample set  $D = \{I^v, I^r, Y\}$ , where  $I^v = \{I_i^v\}_{i=1}^{N_v}$  represents the visible image set,  $I^r = \{I_i^r\}_{i=1}^{N_r}$  is the infrared image set, and  $Y = \{y_i\}_{i=1}^{N_y}$  is the label set. Each  $y_i \in \mathbb{R}^{N_y}$  is a one-hot ground-truth label vector, and  $N_y$  is the number of identities. For a visible-infrared image pair  $(I_i^v, I_i^r)$ , we use ResNet50 [13] as the backbone network to extract visual features. To effectively model modality-specific information, we duplicate the shallow layers of ResNet50 to construct two modality-specific encoders,  $E_v$  and  $E_r$ , which extract low-level features  $v_{v,i}^l$  and  $v_{r,i}^l$  from visible and infrared images, respectively. The remaining layers of ResNet50 serve as a modality-shared encoder  $E$ , which maps the modality-specific low-level features into a joint feature space to learn modality-invariant visual representations  $v_{v,i}$  and  $v_{r,i}$ . Previous studies [24, 58, 66] have highlighted the effectiveness of CLIP [37] in addressing the challenges of ReID, demonstrating that its powerful vision-language joint representation significantly enhances cross-modal matching and semantic understanding. To leverage CLIP's strong capability in high-level semantic comprehension, we initialize our image backbone network using CLIP's visual encoder.

The goal is to align  $v_{v,i}$  and  $v_{r,i}$  in the joint feature space, which requires the encoder to effectively extract modality-shared high-level semantic information from both infrared and visible images.

To achieve this, work [66] employs a vision-language alignment mechanism to generate textual descriptions for infrared and visible images separately, introducing additional semantic supervision to guide the visual encoder in learning key features such as body shape. Although this approach attempts to capture body shape information through textual descriptions, it does not explicitly model body shape features but instead relies on the model to discover them automatically during contrastive learning. However, relying solely on implicit learning may not be sufficient for the model to fully capture and utilize body shape features, thereby limiting its recognition performance. In light of this, we propose BSaTa, which explicitly extracts and utilizes body shape information, thereby enhancing feature representation for VIREID. It primarily consists of a Body Shape Textual Alignment module, equipped with a Text-Visual Consistency Regularizer, and a Shape-aware Representation Learning module.

### 3.2 Body Shape Textual Alignment

Body shape information is inherently modality-invariant and plays a crucial role in VIREID. However, relying solely on identity-level supervision to implicitly learn body shape features from images is highly challenging, as identity information often encompasses multiple appearance factors that may interfere with the extraction of body shape features. To address this issue, a viable approach is to incorporate an advanced human parsing model to obtain body shape maps from images and use them to generate shape features as supervision signals, guiding the network to better capture body shape information [22]. However, since shape features are typically extracted from the parsed body shape maps, their expressiveness is constrained by the semantic understanding capability of the visual network, making it difficult to directly support higher-level semantic comprehension. In recent years, vision-language pretraining models, such as CLIP, have demonstrated powerful high-level semantic extraction capabilities in multimodal learning. By leveraging text as a supervision signal, these models significantly enhance the ability of visual networks to understand complex semantics. Inspired by this, our goal is to obtain textual representations that describe body shape information and use them as supervision signals to help the network more effectively learn shape features, thereby improving the robustness of cross-modality matching and feature representation. However, acquiring high-quality textual descriptions of body shape remains a key challenge. To tackle this, we design a Body Shape Textual Alignment (BSTA) module, equipped with a Text-Visual Consistency Regularizer (TVCR).

**Body Shape Textual Alignment (BSTA) Module.** This module leverages CLIP's strong vision-language alignment capability to transform body shape maps, generated by the human parsing model, into structured textual shape representations. Specifically, given a visible-infrared image pair  $(I_i^v, I_i^r)$ , we employ the advanced human parsing model SCHP [21] to generate the corresponding shape maps  $H_i^v$  and  $H_i^r$ , which are then fed into their respective modality-specific encoding networks for feature extraction. To further refine the representation, we introduce an additional shape encoder  $E_s$ , constructed by duplicating the last block of ResNet50. This encoder functions as a modality-shared module, generating the visual shape features  $v_{v,i}^s$  and  $v_{r,i}^s$ .

After obtaining the visual shape features, we further convert them into modality-aligned textual shape representations based on CLIP. To achieve this, inspired by CLIP-ReID [24], we introduce a learnable textual shape description  $T_i^s$ , formatted as follows:

$$T_i^s = "A photo of a [X_1^s][X_2^s]...[X_M^s][CLS] shape", \quad (1)$$

where  $[X_m^s]$  represents a trainable shape word token,  $[CLS]$  denotes the identity label corresponding to  $(I_i^v, I_i^r)$ , and  $M$  is the total number of learnable shape tokens. This learnable text description is adaptively optimized by aligning it with the corresponding visual shape features, enabling it to more accurately capture the key semantic information of the shape features. We then use CLIP's textual encoder  $E_t$  to extract the textual shape feature  $t_i^s$  from  $T_i^s$ , thereby obtaining a modality-aligned textual shape representation. This textual shape representation  $t_i^s$  is identity-level and modality-invariant, remaining unaffected by variations in illumination, viewpoint, and other factors. Essentially, it serves as a shape prototype. Therefore, we align the textual shape representation  $t_i^s$  with the visual shape features  $(v_{v,i}^s$  and  $v_{r,i}^s)$  using a bidirectional cross-modal contrastive loss, as follows:

$$\mathcal{L}_{bcon}^s = \mathcal{L}_{i2t}^s + \mathcal{L}_{t2i}^s, \quad (2)$$

$$\begin{aligned} \mathcal{L}_{i2t}^s = & -\frac{1}{n_v} \sum_{i=1}^{n_v} \log \frac{\exp(\text{sim}(v_{v,i}^s, t_i^s))}{\sum_{j=1}^{n_v} \exp(\text{sim}(v_{v,j}^s, t_j^s))} \\ & -\frac{1}{n_r} \sum_{i=1}^{n_r} \log \frac{\exp(\text{sim}(v_{r,i}^s, t_i^s))}{\sum_{j=1}^{n_r} \exp(\text{sim}(v_{r,j}^s, t_j^s))}, \end{aligned} \quad (3)$$

$$\begin{aligned} \mathcal{L}_{t2i}^s = & -\frac{1}{n_v} \sum_{i=1}^{n_v} \frac{1}{|P(y_i)|} \sum_{p_i \in P(y_i)} \log \frac{\exp(\text{sim}(v_{v,p_i}^s, t_{y_i}^s))}{\sum_{j=1}^{n_v} \exp(\text{sim}(v_{v,j}^s, t_{y_i}^s))} \\ & -\frac{1}{n_r} \sum_{i=1}^{n_r} \frac{1}{|P(y_i)|} \sum_{p_i \in P(y_i)} \log \frac{\exp(\text{sim}(v_{r,p_i}^s, t_{y_i}^s))}{\sum_{j=1}^{n_r} \exp(\text{sim}(v_{r,j}^s, t_{y_i}^s))} \end{aligned} \quad (4)$$

where  $n_v = n_r$ , and  $\text{sim}(\cdot)$  denotes the cosine similarity function.  $t_{y_i}^s$  is the textual shape feature for identity  $y_i$ , while  $P(y_i)$  represents the set of sample indices corresponding to identity  $y_i$ , with  $|P(y_i)|$  denoting the cardinality of  $P(y_i)$ .

**Text-Visual Consistency Regularizer.** To strengthen text-visual alignment, we introduce a Text-Visual Consistency Regularizer on top of the bidirectional cross-modal contrastive loss, ensuring bidirectional consistency in text-image matching. While the contrastive loss optimizes the relative similarity between positive and negative pairs, it does not explicitly enforce the symmetry of the similarity matrix across modalities, which could lead to unstable matching and inconsistent modality distributions. By incorporating the symmetry constraint, we promote symmetric alignment between images and text in the shared feature space, thereby reducing modality discrepancies. This enables the textual shape representation to more accurately describe the visual shape features and enhances the reliability of the generated textual shape

representation. The text-visual consistency regularizer is formulated as follows:

$$\mathcal{L}_{tvcr}^s = \frac{1}{n_v} \sum_{i=1}^{n_v} \sum_{j=1}^{n_v} (\text{sim}(\mathbf{v}_{v,i}^s, \mathbf{t}_j^s) - \text{sim}(\mathbf{v}_{v,j}^s, \mathbf{t}_i^s))^2 + \frac{1}{n_r} \sum_{i=1}^{n_r} \sum_{j=1}^{n_r} (\text{sim}(\mathbf{v}_{r,i}^s, \mathbf{t}_j^s) - \text{sim}(\mathbf{v}_{r,j}^s, \mathbf{t}_i^s))^2. \quad (5)$$

In this way, we generate dependable textual shape representations that serve as robust semantic descriptions of visual shape features. These textual representations are then used to guide the training of the visual encoder, enabling it to accurately capture identity-related, modality-invariant body shape information. This effectively reduces the modality gap and enhances cross-modal matching performance.

Furthermore, to leverage CLIP's powerful semantic understanding for enhancing the visual encoder's ability to capture modality-shared appearance features, we follow CSDN [66] and introduce a learnable, modality-invariant, identity-level appearance description  $T_i^a = "A photo of a [X_1^a][X_2^a]...[X_N^a][CLS] person"$ , where  $N$  is the total number of learnable shape tokens. This description is then processed by CLIP's textual encoder to extract textual appearance representations. We refer to  $\mathbf{v}_{v,i}$  and  $\mathbf{v}_{r,i}$  as the visual appearance features  $\mathbf{v}_{v,i}^a$  and  $\mathbf{v}_{r,i}^a$ , respectively. Subsequently, we guide the learning of the modality-shared text appearance description using a bidirectional cross-modal alignment loss  $\mathcal{L}_{bcon}^a$ , based on visual appearance features, formulated similarly to Equations (2), (3), and (4). Similarly, the consistency regularizer is applied to the textual appearance representation, denoted as  $\mathcal{L}_{tvcr}^a$ .

### 3.3 Shape-aware Representation Learning

This paper aims to enhance the visual encoder's ability to perceive body shape information, facilitating a more comprehensive extraction of modality-shared features and improving cross-modal matching performance. Unlike traditional methods that rely solely on identity supervision, we draw inspiration from the success of VLP models and leverage the generated textual shape representations as supervisory signals. The signals guide the visual encoder in learning more robust and discriminative body shape features. By explicitly modeling modality-shared shape information in this way, we not only strengthen the model's understanding of high-level semantic features but also effectively reduce modality gaps, thereby improving the robustness and accuracy of cross-modal person re-identification.

Formally, for the visible-infrared image pair  $(I_i^v, I_i^r)$ , we use the generated identity-level textual shape descriptions as supervisory signals to optimize the backbone network  $(E_v, E_r, E)$  and shape encoder  $E_s$ . Additionally, we leverage the generated textual appearance descriptions to supervise the optimization of the backbone network, promoting the exploration of shared appearance features across modalities. Together, these form a multi-text supervision mechanism that steers the model's optimization, enabling it to accurately capture identity-related key information across different modalities. This further reduces modality discrepancies and enhances feature discriminability. The corresponding optimization

loss is defined as follows:

$$\mathcal{L}_{i2tce}^a = -\frac{1}{n_v} \sum_{i=1}^{n_v} \mathbf{y}_i \log \frac{\exp(\text{sim}(\mathbf{v}_{v,i}^a, \mathbf{t}_{y_i}^a))}{\sum_{y_j=1}^{N_y} \exp(\text{sim}(\mathbf{v}_{v,i}^a, \mathbf{t}_{y_j}^a))} - \frac{1}{n_r} \sum_{i=1}^{n_r} \mathbf{y}_i \log \frac{\exp(\text{sim}(\mathbf{v}_{r,i}^a, \mathbf{t}_{y_i}^a))}{\sum_{y_j=1}^{N_y} \exp(\text{sim}(\mathbf{v}_{r,i}^a, \mathbf{t}_{y_j}^a))}, \quad (6)$$

$$\mathcal{L}_{i2tce}^s = -\frac{1}{n_v} \sum_{i=1}^{n_v} \mathbf{y}_i \log \frac{\exp(\text{sim}(\mathbf{v}_{v,i}^s, \mathbf{t}_{y_i}^s))}{\sum_{y_j=1}^{N_y} \exp(\text{sim}(\mathbf{v}_{v,i}^s, \mathbf{t}_{y_j}^s))} - \frac{1}{n_r} \sum_{i=1}^{n_r} \mathbf{y}_i \log \frac{\exp(\text{sim}(\mathbf{v}_{r,i}^s, \mathbf{t}_{y_i}^s))}{\sum_{y_j=1}^{N_y} \exp(\text{sim}(\mathbf{v}_{r,i}^s, \mathbf{t}_{y_j}^s))}, \quad (7)$$

where  $N_y$  is the total number of identities. By leveraging this multi-text supervision strategy, we not only utilize the prior knowledge of CLIP [37], but also enhance the network's ability to understand and model modality-invariant shape and appearance information. This explicit modeling approach effectively directs the network to focus on identity-related, modality-invariant features, thereby improving the performance of VIREID.

**Distribution Consistency Constraint.** The losses outlined above guide the network to capture modality-shared identity information by aligning the visual features with their corresponding textual prototypes. To further reduce the distribution gap between cross-modal features, we use identity-level textual representations as reference centers for modality alignment and construct a text-based distribution consistency constraint across modalities. Specifically, for the visible-infrared visual features  $(\mathbf{v}_i^v, \mathbf{v}_i^r)$  and textual prototype set  $T_p = \{\mathbf{t}_j\}_{j=1}^{N_y} \in \mathbb{R}^{N_y \times d}$ , we compute the similarity probability distribution  $p_{i,j}$  of  $\mathbf{v}_i$  and  $\mathbf{t}_j$  as follows:

$$p_{i,j} = \frac{\exp(\text{sim}(\mathbf{v}_i, \mathbf{t}_j))}{\sum_{k=1}^{N_y} \exp(\text{sim}(\mathbf{v}_i, \mathbf{t}_k))}, \quad (8)$$

where  $\mathbf{v}_i = \{\mathbf{v}_i^v, \mathbf{v}_i^r\}$ . When  $\mathbf{v}_i$  is set to  $\mathbf{v}_i^v$  and  $\mathbf{v}_i^r$  respectively, we obtain  $p_{i,j}^v$  and  $p_{i,j}^r$ . We expect the similarity probability distribution between image features from the visible and infrared modalities and textual prototypes to remain consistent, thereby enhancing cross-modal alignment. This constraint is formulated as follows:

$$\mathcal{L}_{dcc} = \frac{1}{n} \sum_{i=1}^n \sum_{j=1}^{N_y} (p_{i,j}^v - p_{i,j}^r)^2, \quad (9)$$

where  $n = n_v = n_r$ . We apply the above constraint to both the shape textual representation  $\mathbf{t}_j^s$  and the appearance textual representation  $\mathbf{t}_j^a$ , denoted as  $\mathcal{L}_{dcc}^s$  and  $\mathcal{L}_{dcc}^a$ , respectively. Due to the modality-invariant nature and strong semantic abstraction capability of textual representations, this "distribution-consistent alignment" strategy guides the network to learn modality-shared identity representations without disrupting the intrinsic feature structures of each modality. By enforcing such geometric consistency constraints, we achieve more robust cross-modal identity alignment in the latent semantic space, improving both matching accuracy and the model's generalization ability.

### 3.4 Training and Inference

The optimization of BSaTa is divided into two stages to ensure the reliability of shape and appearance features while enhancing cross-modal matching performance. In the first stage, we focus on optimizing the learnable textual shape and appearance descriptions  $T_i^s$  and  $T_i^a$ , while freezing the backbone network and shape encoder. The loss function  $\mathcal{L}^{s1} = \mathcal{L}_{bcon}^s + \mathcal{L}_{bcon}^a + \lambda_1(\mathcal{L}_{tvcr}^s + \mathcal{L}_{tvcr}^a)$  is employed to refine the learnable word tokens, enabling them to accurately capture modality-shared shape and appearance information, thereby generating robust and semantically rich textual representations.

In the second stage, the generated shape and appearance descriptions are frozen, while the backbone network ( $E_v$ ,  $E_r$ ,  $E$ ) and shape encoder  $E_s$  are unfrozen for further optimization. In addition to using textual shape and appearance supervision to refine the visual encoder, we also follow [66] and incorporate identity information as an additional supervision signal to enhance the modeling of identity-related features. This includes the identity loss ( $\mathcal{L}_{id}$ ) and the weighted regularized triplet loss ( $\mathcal{L}_{wrt}$ ) [64]. Thus, the overall objective function for the second stage is formulated as:

$$\mathcal{L}^{s2} = \mathcal{L}_{id} + \lambda_2 \mathcal{L}_{wrt} + \lambda_3 (\mathcal{L}_{i2tce}^a + \mathcal{L}_{i2tce}^s) + \lambda_4 (\mathcal{L}_{dec}^s + \mathcal{L}_{dec}^a), \quad (10)$$

where  $\lambda_1$ ,  $\lambda_2$ ,  $\lambda_3$ , and  $\lambda_4$  balance the contribution of different losses.

The learnable textual descriptions, CLIP's text encoder, and the semantic parsing model are used exclusively during training to obtain reliable textual descriptions that provide supervision for the visual encoder. These components are removed during inference. During inference, the corresponding appearance and body shape features are extracted from both infrared and visible images. These features are then concatenated, and their cosine similarity score is computed as the retrieval criterion.

## 4 EXPERIMENTS

### 4.1 Experiment Settings

**Datasets and Metrics:** To evaluate the effectiveness of our approach, we conduct experiments on two VIReID datasets. **SYSU-MM01** [52] is a challenging dataset specifically designed for VIReID, containing 491 identities, with a total of 287,628 visible images and 15,792 infrared images captured using 4 visible-light cameras and 2 infrared cameras in both indoor and outdoor environments. Following the standard evaluation protocol [52], the training set consists of 395 identities with 22,258 visible and 11,909 infrared images, while the test set includes 96 identities. The dataset supports two retrieval settings: all-search mode, which includes visible images from both indoor and outdoor cameras, and indoor-search mode, where only indoor camera images are considered. Additionally, testing can be conducted under single-shot and multi-shot gallery settings, where each identity is represented by either 1 or 10 visible images, respectively. **RegDB** [34] is a smaller dataset consisting of 8,240 images from 412 identities, with each identity having 10 visible and 10 infrared images captured from a single paired-camera setup. Following the protocol in [44], 206 identities are randomly selected for training, while the remaining 206 identities form the test set. The dataset allows evaluation in two cross-modal retrieval directions: visible-to-infrared and infrared-to-visible person retrieval.

To ensure a fair comparison, each experiment is repeated across 10 random training/testing splits, and the final results are reported as the average over all runs.

For performance evaluation, we adopt standard retrieval metrics, including the Cumulative Matching Characteristics (CMC) curve and mean Average Precision (mAP). Specifically, we report R@1, R@10, and R@20 accuracy to measure retrieval effectiveness at different ranks.

**Implementation Details:** For input images, we uniformly resize them to 288×144 and apply standard data augmentation techniques, including random flipping, padding, and cropping, to enhance generalization. Our model adopts CLIP [37] as the backbone, incorporating two parallel shallow branches for modality-specific feature extraction, while the remaining four deep convolutional blocks are shared to capture modality-invariant representations. The number of learnable word tokens in the shape and appearance descriptions is set to 4 for both  $M$  and  $N$ . The hyperparameters for different loss components are set as  $\lambda_1 = 0.04$ ,  $\lambda_2 = 0.15$ ,  $\lambda_3 = 0.05$  and  $\lambda_4 = 0.05$  to effectively balance the training objectives. Model training utilizes the Adam optimizer with a weight decay factor of 4e-5. The training process is divided into two stages, each with distinct optimization strategies. In the first stage, we train two learnable texts for 60 epochs with an initial learning rate of  $3 \times 10^{-4}$ , following a cosine annealing schedule [24] for gradual decay. In the second stage, we fine-tune the backbone network and shape encoder for 120 epochs. The learning rate is linearly warmed up from  $3 \times 10^{-6}$  to  $3 \times 10^{-4}$  over the first 10 epochs and then decayed by a factor of 0.1 at epochs 40 and 70. The training batch size is set to 64, consisting of 8 identities, with each identity represented by 4 visible and 4 infrared images. We implement our method using PyTorch library and conduct all experiments on a single NVIDIA GTX3090 24GB GPU.

### 4.2 Comparisons with State-of-the-art Models

In this section, we compare our proposed BSaTa framework with the current state-of-the-art (SOTA) methods on two VIReID datasets, as shown in Tables 1 and 2. The compared methods are categorized into two groups: generative and non-generative approaches. As observed from the tables, non-generative methods significantly outperform generative ones and currently dominate the VIReID task. Our BSaTa belongs to the non-generative category.

Table 1 presents the performance comparison with SOTA methods on **SYSU-MM01**. The proposed BSaTa framework achieves competitive results across all evaluation metrics and settings. Notably, in the commonly used AS-SS (All-Search, Single-Shot) mode, our method achieves SOTA performance, with an impressive R@1 accuracy of 77.4% and mAP of 74.3%. Compared to the runner-up method CSDN [66], BSaTa improves by 0.7% in R@1 and 1.3% in mAP. The key difference between BSaTa and CSDN lies in the explicit incorporation of body shape information, and the significant performance gain highlights the effectiveness of our method and the importance of shape information in VIReID. Our approach also performs well in other settings, achieving the highest mAP under AS-MS (All-Search, Multi-Shot), IS-SS (Indoor-Search, Single-Shot), and IS-MS (Indoor-Search, Multi-Shot) modes with scores of 69.6%, 87.1%, and 83.2%, respectively, further demonstrating the robustness and superiority of BSaTa. Table 2 presents the comparison

**Table 1: Performance comparison with state-of-the-art methods on SYSU-MM01. ‘-’ denotes that no reported result is available.**

Methods	Venue	All-Search				Indoor-Search			
		Single-Shot		Multi-Shot		Single-Shot		Multi-Shot	
		R@1	mAP	R@1	mAP	R@1	mAP	R@1	mAP
Hi-CMD [4]	CVPR’20	34.9	35.9	-	-	-	-	-	-
JSIA [45]	AAAI’20	38.1	36.9	45.1	29.5	43.8	52.9	52.7	42.7
X-Modality [17]	AAAI’20	49.9	50.7	-	-	-	-	-	-
MSA [33]	IJCAT’21	63.1	59.2	-	-	67.1	72.7	-	-
CECNet [72]	TCSV’22	53.3	51.8	-	-	60.6	62.8	-	-
RBDF [50]	TCYB’22	57.6	54.4	-	-	-	-	-	-
TSME [27]	TCSV’22	64.2	61.2	70.3	54.3	64.8	71.3	76.8	65.0
ACD [35]	TIFS’24	74.4	71.1	80.4	66.9	78.9	82.7	86.0	78.6
AGP <sup>2</sup> [1]	TIFS’25	72.2	70.5	-	-	83.4	84.2	-	-
AGW [64]	TPAMI’21	47.5	47.6	-	-	54.1	62.9	-	-
MSO [11]	MM’21	58.7	56.4	65.8	49.5	63.0	70.3	72.0	61.6
MPANet [54]	CVPR’21	70.5	68.2	75.5	62.9	76.7	80.9	84.2	75.1
MMN [71]	MM’21	70.6	66.9	-	-	76.2	79.6	-	-
FMCNet [69]	CVPR’22	66.3	62.5	73.4	56.0	68.1	74.0	78.8	63.8
DART [62]	CVPR’22	68.7	66.2	-	-	72.5	78.1	-	-
DCLNet [39]	MM’22	70.8	65.3	-	-	73.5	76.8	-	-
MAUM [26]	CVPR’22	71.6	68.7	-	-	76.9	81.9	-	-
PMT [29]	AAAI’23	67.5	64.9	-	-	71.6	76.5	-	-
ProtoHPE [67]	MM’23	71.9	70.5	-	-	77.8	81.3	-	-
CAL [53]	ICCV’23	74.6	71.7	77.0	64.8	79.6	83.6	86.9	78.5
MBCE [3]	AAAI’23	74.7	72.0	78.3	65.7	83.4	86.0	88.4	80.6
SEFL [10]	CVPR’23	75.1	70.1	-	-	78.4	81.2	-	-
PMWGCN [40]	TIFS’24	66.8	64.8	-	-	72.6	76.1	-	-
DARD [51]	TIFS’24	69.3	65.7	-	-	79.6	60.3	-	-
CAJ <sub>+</sub> [65]	TPAMI’24	71.4	68.1	-	-	78.4	82.0	-	-
RLE [41]	NeurIPS’24	75.4	72.4	-	-	84.7	87.0	-	-
HOS-Net [36]	AAAI’24	75.6	74.2	-	-	84.2	86.7	-	-
AMINet [15]	arXiv’25	74.7	66.1	-	-	79.1	82.3	-	-
CSCL [28]	TMM’25	75.7	72.0	-	-	80.8	83.5	-	-
ScRL [22]	PR’25	76.1	72.6	-	-	82.4	85.4	-	-
DMPF [31]	TNNLS’25	76.4	71.5	-	-	82.2	84.9	-	-
CycleTrans [55]	TNNLS’25	76.5	72.6	82.8	68.5	87.2	84.9	91.2	81.4
CSDN [66]	TMM’25	76.7	73.0	83.5	67.9	84.5	86.8	91.3	82.2
BSaTa (Ours)	-	77.4	74.3	83.2	69.6	84.7	87.1	91.0	83.2

results on **RegDB**. Our BSaTa establishes new SOTA performance for visible-to-infrared retrieval, with an R@1 of 95.8% and mAP of 89.1%. For infrared-to-visible retrieval, our method achieves competitive performance, being only 0.1% lower in R@1 compared to MBCE [3]. In summary, BSaTa consistently achieves superior performance across both datasets. This success can be attributed to the effective use of body shape information, which enables the model to extract highly discriminative and modality-invariant identity features.

### 4.3 Ablation Studies

We conduct ablation experiments for BSaTa on SYSU-MM01 under the AS-SS setting.

**Contributions of Proposed Components:** Table 3 presents a comprehensive ablation study evaluating the effectiveness of each component in our BSaTa, including Appearance-Textual Alignment (ATA), Appearance-Aware Representation Learning (AARL), Body Shape-Textual Alignment (BSTA), Text-Visual Consistency Regularization (TVCR), Shape-Aware Representation Learning (SARL), and Distribution Consistency Constraint (DCC).

The baseline model (0#) refers to the backbone network trained solely with identity loss ( $\mathcal{L}_{id}$ ) and the weighted regularized triplet loss ( $\mathcal{L}_{wrt}$ ), achieving an R@1 accuracy of 68.2% and a mAP of 64.9%. When textual appearance descriptions are introduced in Baseline (1#), leveraging CLIP to enhance the backbone’s ability to model high-level semantic appearance features, the performance experiences a significant boost, with R@1 and mAP increasing by 6.8% and 7.0%, respectively. Replacing textual appearance with textual shape descriptions (2#) also yields a considerable improvement, achieving 75.2% R@1 and 71.8% mAP, highlighting the crucial role of shape information in VIREID. When both textual appearance and shape descriptions are jointly utilized (3#), a multi-text supervision mechanism is formed, leading to further performance enhancement, with gains of 1.0% in R@1 and 1.6% in mAP. Building upon this, the addition of the TVCR module (4#) effectively strengthens visual-textual semantic alignment and ensures the reliability of the generated text embeddings, thereby contributing to improved discriminative capability. Similarly, incorporating the DCC module (5#) on top of 3# enables alignment of feature distributions between infrared and visible modalities using text embeddings as semantic anchors. This facilitates the extraction of modality-invariant

**Table 2: Performance comparison with state-of-the-art methods on RegDB.**

Methods	Venue	Visible to Infrared		Infrared to Visible	
		R@1	mAP	R@1	mAP
JSIA [45]	AAAI'20	48.5	49.3	48.1	48.9
Hi-CMD [4]	CVPR'20	70.9	66.0	-	-
X-Modality [17]	AAAI'20	-	-	62.2	60.1
MSA [33]	IJCAI'21	84.8	82.1	-	-
RBDFF [50]	TCYB'22	79.8	76.7	76.2	73.9
CECNet [72]	TCSVT'22	82.3	78.4	78.9	75.5
TSME [27]	TCSVT'22	87.3	76.9	86.4	75.7
ACD [35]	TIFS'24	84.7	83.2	87.1	84.7
AGPI <sup>2</sup> [1]	TIFS'25	89.0	83.8	87.9	83.0
AGW [64]	TPAMI'21	70.0	66.3	70.4	65.9
MSO [11]	MM'21	73.6	66.9	74.6	67.5
MPANet [54]	CVPR'21	83.7	80.9	82.8	80.7
MMN [71]	MM'21	91.6	84.1	87.5	80.5
DCLNet [39]	MM'22	81.2	74.3	78.0	70.6
DART [62]	CVPR'22	83.6	60.6	81.9	56.7
MAUM [26]	CVPR'22	87.8	85.0	86.9	84.3
FMCNet [69]	CVPR'22	89.1	84.4	88.3	83.8
PMT [29]	AAAI'23	84.8	76.5	84.1	75.1
ProtoHPE [67]	MM'23	88.7	83.7	88.6	81.9
SEFL [10]	CVPR'23	91.0	85.2	92.1	86.5
MBCE [3]	AAAI'23	93.1	88.3	93.4	87.9
CAJ <sub>+</sub> [65]	TPAMI'24	85.6	79.7	84.8	78.5
DARD [51]	TIFS'24	86.2	85.4	85.5	85.1
PMWGCN [40]	TIFS'24	90.6	84.5	88.7	81.6
RLE [41]	NeurIPS'24	92.8	88.6	91.0	86.6
DMPF [31]	TNNLS'25	88.8	81.0	88.8	81.8
CycleTrans [55]	TNNLS'25	90.6	85.6	81.8	87.0
AMINet [15]	arXiv'25	91.2	84.6	89.5	82.4
CSCL [28]	TMM'25	92.1	84.2	89.6	85.0
SeRL [22]	PR'25	92.4	86.7	91.8	85.3
CSDN [66]	TMM'25	95.4	87.7	92.3	85.5
BSaTa (Ours)	-	95.8	89.1	93.3	87.9

**Table 3: Effectiveness of different components on SYSU-MM01.**

No.	ATA	AARL	BSTA	TVCR	SARL	DCC	R@1	mAP
0#							68.2	64.9
1#	✓	✓					75.0	71.9
2#			✓		✓		75.2	71.8
3#	✓	✓	✓		✓		76.2	73.4
4#	✓	✓	✓	✓	✓		76.8	74.1
5#	✓	✓	✓		✓	✓	76.9	73.8
6#	✓	✓	✓	✓	✓	✓	77.4	74.3

identity features, resulting in more robust performance. Ultimately, when all modules are jointly applied (6#), our BSaTa framework achieves the best overall performance across all metrics, demonstrating the synergy between components and the effectiveness of our complete design in addressing the VIREID task.

**Table 4: Effects of learnable word token lengths  $M$  and  $N$  on SYSU-MM01.**

Method	R@1	R@10	R@20	mAP
$M = 2$	76.4	97.5	99.5	73.4
$M = 4$ (Ours)	77.4	97.5	99.4	74.3
$M = 6$	76.4	97.7	99.5	73.4
$M = 8$	76.0	97.4	99.3	73.5
$N = 2$	76.4	97.5	99.3	73.4
$N = 4$ (Ours)	77.4	97.5	99.4	74.3
$N = 6$	76.5	97.6	99.4	73.6
$N = 8$	76.9	97.2	99.1	73.3

**Impact of learnable word token lengths  $M$  and  $N$ :** The lengths of learnable word tokens,  $M$  and  $N$ , for textual shape and appearance descriptions are critical parameters that influence the quality of the textual representations. To investigate their impact, we vary  $M$  and  $N$  in the range of 2, 4, 6, 8 and report the results in Table 4. The observed trend indicates that larger values of  $M$  and  $N$  generally lead to better performance, as they provide richer contextual information for capturing appearance and shape features. Notably, the model achieves peak performance with an R@1 accuracy of 77.4% when both  $M$  and  $N$  are set to 4. However, excessively large values may introduce redundant information, leading to overfitting and increased computational cost. Therefore, we adopt  $M = N = 4$  as a trade-off between performance and efficiency.

**Table 5: Effect of TVCR and DCC on SYSU-MM01.**

Method	R@1	R@10	R@20	mAP
Base (3#)	76.2	96.5	98.3	73.4
TVCR-A	76.4	96.9	98.7	73.7
TVCR-S	76.5	97.1	98.5	73.6
TVCR-SA (Ours)	76.8	97.5	99.3	74.1
DCC-A	76.7	97.2	99.1	74.0
DCC-S	76.4	96.8	98.9	73.8
DCC-SA (Ours)	76.9	97.3	99.3	73.8

**Effect of TVCR and DCC:** In this section, we evaluate the effectiveness of the Text-Visual Consistency Regularizer (TVCR) and the Distribution Consistency Constraint (DCC), as shown in Table 5. Specifically, based on model 3# in Table 3, we examine the performance impact of applying these modules individually to either the appearance or shape textual representations, as well as simultaneously to both. The results show that applying TVCR or DCC to a single textual representation yields distinct performance gains, confirming the effectiveness of our proposed modules. Furthermore, the best performance is achieved when both modules are applied together to both textual shape and appearance representations.

## 5 CONCLUSION

In this paper, we proposed an effective Body Shape-aware Textual Alignment (BSaTa) framework to address the modality gap and semantic limitations in VIREID. Unlike prior works that overlook the importance of body shape information, our approach explicitly models and leverages body shape cues through structured textual representations. The proposed BSTA module effectively extracts body shape semantics using human parsing and CLIP-based encoding, while the TVCR ensures alignment between textual and visual body shape features. Furthermore, the integration of Shape-aware Representation Learning (SRL), incorporating multi-text supervision and distribution consistency constraint, enables the visual encoder to learn more discriminative and modality-invariant identity representations. Extensive experiments on the SYSU-MM01 and RegDB datasets demonstrate that our method achieves superior performance, validating the effectiveness of body shape modeling and our BSaTa. In the future, we plan to explore more fine-grained and dynamic textual guidance to further enhance VIREID.

## REFERENCES

[1] Mahdi Alehdaghi, Arthur Josi, Rafael M. O. Cruz, Pourya Shamsolmoali, and Eric Granger. 2025. Adaptive Generation of Privileged Intermediate Information for Visible-Infrared Person Re-Identification. *IEEE Transactions on Information Forensics and Security* 20 (2025), 3400–3413.

[2] Yen-Chun Chen, Linjie Li, Licheng Yu, Ahmed El Kholy, Faisal Ahmed, Zhe Gan, Yu Cheng, and Jingjing Liu. 2020. UNITER: UNiversal Image-TExt Representation Learning. In *European Conference on Computer Vision (ECCV)*. 104–120.

[3] De Cheng, Xiaolong Wang, Nannan Wang, Zhen Wang, Xiaoyu Wang, and Xinbo Gao. 2023. Cross-modality person re-identification with memory-based contrastive embedding. In *AAAI conference on artificial intelligence (AAAI)*, Vol. 37. 425–432.

[4] Seocheon Choi, Sumin Lee, Youngeun Kim, Taekyung Kim, and Changick Kim. 2020. Hi-CMD: Hierarchical cross-modality disentanglement for visible-infrared person re-identification. In *IEEE conference on computer vision and pattern recognition (CVPR)*. 10257–10266.

[5] Jia Deng, Wei Dong, Richard Socher, Li-Jia Li, Kai Li, and Fei-Fei Li. 2009. ImageNet: A large-scale hierarchical image database. In *IEEE Conference on Computer Vision and Pattern Recognition (CVPR)*. 248–255.

[6] Neng Dong, Shuanglin Yan, Hao Tang, Jinhui Tang, and Liyan Zhang. 2024. Multi-view Information Integration and Propagation for occluded person re-identification. *Information Fusion* 104 (2024), 102201.

[7] Neng Dong, Shuanglin Yan, Liyan Zhang, and Jinhui Tang. 2024. Embedding and Enriching Explicit Semantics for Visible-Infrared Person Re-Identification. *arXiv preprint arXiv:2412.08406* (2024).

[8] Neng Dong, Liyan Zhang, Shuanglin Yan, Hao Tang, and Jinhui Tang. 2024. Erasing, Transforming, and Noising Defense Network for Occluded Person Re-Identification. *IEEE Transactions on Circuits and Systems for Video Technology* 34, 6 (2024), 4458–4472.

[9] Alexey Dosovitskiy, Lucas Beyer, Alexander Kolesnikov, Dirk Weissenborn, Xiaohua Zhai, Thomas Unterthiner, Mostafa Dehghani, Matthias Minderer, Georg Heigold, Sylvain Gelly, Jakob Uszkoreit, and Neil Houlsby. 2021. An Image is Worth 16x16 Words: Transformers for Image Recognition at Scale. In *International Conference on Learning Representations (ICLR)*.

[10] Jiawei Feng, Ancong Wu, and Wei-Shi Zheng. 2023. Shape-Erased Feature Learning for Visible-Infrared Person Re-Identification. In *IEEE Conference on Computer Vision and Pattern Recognition (CVPR)*. 22752–22761.

[11] Yajun Gao, Tengfei Liang, Yi Jin, Xiaoyan Gu, Wu Liu, Yidong Li, and Congyan Lang. 2021. MSO: Multi-feature space joint optimization network for rgb-infrared person re-identification. In *ACM international conference on multimedia (ACM MM)*. 5257–5265.

[12] Ian Goodfellow, Jean Pouget-Abadie, Mehdi Mirza, Bing Xu, David Warde-Farley, Sherjil Ozair, Aaron Courville, and Yoshua Bengio. 2020. Generative adversarial networks. *Commun. ACM* 63, 11 (2020), 139–144.

[13] Kaiming He, Xiangyu Zhang, Shaoqing Ren, and Jian Sun. 2016. Deep Residual Learning for Image Recognition. In *IEEE Conference on Computer Vision and Pattern Recognition (CVPR)*. 770–778.

[14] Chao Jia, Yinfei Yang, Ye Xia, Yi-Ting Chen, Zarana Parekh, Hieu Pham, Quoc V. Le, Yun-Hsuan Sung, Zhen Li, and Tom Duerig. 2021. Scaling Up Visual and Vision-Language Representation Learning With Noisy Text Supervision. In *International Conference on Machine Learning (ICML)*. 4904–4916.

[15] Yuheng Jia and Wesley Armour. 2025. Adaptive Illumination-Invariant Synergistic Feature Integration in a Stratified Granular Framework for Visible-Infrared Re-Identification. *arXiv preprint arXiv:2502.21163* (2025).

[16] Zhengbao Jiang, Frank F Xu, Jun Araki, and Graham Neubig. 2020. How can we know what language models know? *Transactions of the Association for Computational Linguistics* 8 (2020), 423–438.

[17] Diangang Li, Xing Wei, Xiaopeng Hong, and Yihong Gong. 2020. Infrared-visible cross-modal person re-identification with an x modality. In *AAAI conference on artificial intelligence (AAAI)*, Vol. 34. 4610–4617.

[18] Huafeng Li, Shuanglin Yan, Zhengtao Yu, and Dapeng Tao. 2019. Attribute-identity embedding and self-supervised learning for scalable person re-identification. *IEEE Transactions on Circuits and Systems for Video Technology* 30, 10 (2019), 3472–3485.

[19] Junnan Li, Ramprasaath Selvaraju, Akhilesh Gotmare, Shafiq Joty, Caiming Xiong, and Steven Chu Hong Hoi. 2021. Align before fuse: Vision and language representation learning with momentum distillation. *Advances in neural information processing systems (NeurIPS)* 34 (2021), 9694–9705.

[20] Liunian Harold Li, Mark Yatskar, Da Yin, Cho-Jui Hsieh, and Kai-Wei Chang. 2019. VisualBERT: A Simple and Performant Baseline for Vision and Language. *arXiv* (2019).

[21] Peike Li, Yunqiu Xu, Yunchao Wei, and Yi Yang. 2022. Self-Correction for Human Parsing. *IEEE Transactions on Pattern Analysis and Machine Intelligence* 44, 6 (2022), 3260–3271.

[22] Shuang Li, Jiaxu Leng, Ji Gan, Mengjincheng Mo, and Xinbo Gao. 2023. Shape-centered Representation Learning for Visible-Infrared Person Re-identification. *arXiv preprint arXiv:2310.17952* (2023).

[23] Shuang Li, Fan Li, Jinxing Li, Huafeng Li, Bob Zhang, Dapeng Tao, and Xinbo Gao. 2023. Logical Relation Inference and Multiview Information Interaction for Domain Adaptation Person Re-Identification. *IEEE Transactions on Neural Networks and Learning Systems* (2023).

[24] Siyuan Li, Li Sun, and Qingli Li. 2023. Clip-reid: Exploiting vision-language model for image re-identification without concrete text labels. In *AAAI Conference on Artificial Intelligence (AAAI)*, Vol. 37. 1405–1413.

[25] Xinyu Lin, Jinxing Li, Zeyu Ma, Huafeng Li, Shuang Li, Kaixiong Xu, Guangming Lu, and David Zhang. 2022. Learning modal-invariant and temporal-memory for video-based visible-infrared person re-identification. In *IEEE Conference on Computer Vision and Pattern Recognition (CVPR)*. 20973–20982.

[26] Jialun Liu, Yifan Sun, Feng Zhu, Hongbin Pei, Yi Yang, and Wenhui Li. 2022. Learning memory-augmented unidirectional metrics for cross-modality person re-identification. In *IEEE Conference on Computer Vision and Pattern Recognition (CVPR)*. 19366–19375.

[27] Jianan Liu, Jialiang Wang, Nianchang Huang, Qiang Zhang, and Jungong Han. 2022. Revisiting modality-specific feature compensation for visible-infrared person re-identification. *IEEE Transactions on Circuits and Systems for Video Technology* 32, 10 (2022), 7226–7240.

[28] Min Liu, Zhu Zhang, Yuan Bian, Xueping Wang, Yeqing Sun, Baida Zhang, and Yaonan Wang. 2025. Cross-Modality Semantic Consistency Learning for Visible-Infrared Person Re-Identification. *IEEE Transactions on Multimedia* 27 (2025), 568–580.

[29] Hu Lu, Xuezhang Zou, and Pingping Zhang. 2023. Learning progressive modality-shared transformers for effective visible-infrared person re-identification. In *AAAI Conference on Artificial Intelligence (AAAI)*, Vol. 37. 1835–1843.

[30] Jiasen Lu, Dhruv Batra, Devi Parikh, and Stefan Lee. 2019. ViLBERT: Pretraining Task-Agnostic Visiolinguistic Representations for Vision-and-Language Tasks. In *Advances in Neural Information Processing Systems (NeurIPS)*, Vol. 32.

[31] Zefeng Lu, Ronghao Lin, and Haifeng Hu. 2025. Disentangling Modality and Posture Factors: Memory-Attention and Orthogonal Decomposition for Visible-Infrared Person Re-Identification. *IEEE Transactions on Neural Networks and Learning Systems* 36, 3 (2025), 5494–5508.

[32] Huaishao Luo, Lei Ji, Ming Zhong, Yang Chen, Wen Lei, Nan Duan, and Tianrui Li. 2022. CLIP4Clip: An Empirical Study of CLIP for End to End Video Clip Retrieval. *Neurocomputing* 508 (2022), 293–304.

[33] Ziling Miao, Hong Liu, Wei Shi, Wanlu Xu, and Hanrong Ye. 2021. Modality-aware Style Adaptation for RGB-Infrared Person Re-Identification. In *International Joint Conference on Artificial Intelligence (IJCAI)*. 916–922.

[34] Dat Tien Nguyen, Hyung Gil Hong, Ki Wan Kim, and Kang Ryoung Park. 2017. Person recognition system based on a combination of body images from visible light and thermal cameras. *Sensors* 17, 3 (2017), 605.

[35] Honghu Pan, Wenjie Pei, Xin Li, and Zhenyu He. 2024. Unified Conditional Image Generation for Visible-Infrared Person Re-Identification. *IEEE Transactions on Information Forensics and Security* 19 (2024), 9026–9038.

[36] Liuxiang Qiu, Si Chen, Yan Yan, Jing-Hao Xue, Da-Han Wang, and Shunzhi Zhu. 2024. High-order structure based middle-feature learning for visible-infrared person re-identification. In *AAAI Conference on Artificial Intelligence (AAAI)*, Vol. 38. 4596–4604.

[37] Alex Radford, Jong Wook Kim, Chris Hallacy, Aditya Ramesh, Gabriel Goh, Sandhini Agarwal, Girish Sastry, Amanda Askell, Pamela Mishkin, Jack Clark, Gretchen Krueger, and Ilya Sutskever. 2021. Learning Transferable Visual Models From Natural Language Supervision. In *International Conference on Machine Learning (ICML)*, Vol. 139. 8748–8763.

[38] Taylor Shin, Yasaman Razeghi, Robert L. Logan IV, Eric Wallace, and Sameer Singh. 2020. AutoPrompt: Eliciting Knowledge from Language Models with Automatically Generated Prompts. In *Conference on Empirical Methods in Natural Language Processing (EMNLP)*. 4222–4235.

[39] Hanzhe Sun, Jun Liu, Zhizhong Zhang, Chengjie Wang, Yanyun Qu, Yuan Xie, and Lizhuang Ma. 2022. Not all pixels are matched: Dense contrastive learning for cross-modality person re-identification. In *ACM International Conference on Multimedia (ACM MM)*. 5333–5341.

[40] Rui Sun, Long Chen, Lei Zhang, Ruirui Xie, and Jun Gao. 2024. Robust Visible-Infrared Person Re-Identification Based on Polymorphic Mask and Wavelet Graph Convolutional Network. *IEEE Transactions on Information Forensics and Security* 19 (2024), 2800–2813.

[41] Lei Tan, Yukang Zhang, Keke Han, Pingyang Dai, Yan Zhang, YONGJIAN WU, and Rongrong Ji. 2024. RLE: A Unified Perspective of Data Augmentation for Cross-Spectral Re-Identification. *Advances in Neural Information Processing Systems (NeurIPS)* 37, 126977–126996.

[42] Hao Tang, Jun Liu, Shuanglin Yan, Rui Yan, Zechao Li, and Jinhui Tang. 2023. M3Net: Multi-view Encoding, Matching, and Fusion for Few-shot Fine-grained Action Recognition. In *ACM International Conference on Multimedia (ACM MM)*. 1719–1728.

[43] Kaiyang Zhou, Jingkang Yang, Chen Change Loy, and Ziwei Liu. 2022. Conditional prompt learning for vision-language models. In *IEEE Conference on Computer Vision and Pattern Recognition (CVPR)*. 16816–16825.

[44] Guan'an Wang, Tianzhu Zhang, Jian Cheng, Si Liu, Yang Yang, and Zengguang Hou. 2019. RGB-infrared cross-modality person re-identification via joint pixel and feature alignment. In *IEEE International Conference on Computer Vision (ICCV)*. 3623–3632.

[45] Guan-An Wang, Tianzhu Zhang, Yang Yang, Jian Cheng, Jianlong Chang, Xu Liang, and Zeng-Guang Hou. 2020. Cross-modality paired-images generation for RGB-infrared person re-identification. In *AAAI conference on artificial intelligence (AAAI)*, Vol. 34. 12144–12151.

[46] Wenhui Wang, Hangbo Bao, Li Dong, Johan Bjorck, Zhiliang Peng, Qiang Liu, Kriti Aggarwal, Owais Khan Mohammed, Saksham Singhal, Subhrojit Som, et al. 2023. Image as a Foreign Language: BEiT Pretraining for Vision and Vision-Language Tasks. In *IEEE Conference on Computer Vision and Pattern Recognition (CVPR)*. 19175–19186.

[47] Yang Wang, Jinjia Peng, Huibing Wang, and Meng Wang. 2022. Progressive learning with multi-scale attention network for cross-domain vehicle re-identification. *Science China Information Sciences* 65, 6 (2022). 160103.

[48] Yiming Wang, Guanqiu Qi, Shuang Li, Yi Chai, and Huafeng Li. 2022. Body part-level domain alignment for domain-adaptive person re-identification with transformer framework. *IEEE Transactions on Information Forensics and Security* 17 (2022). 3321–3334.

[49] Zhaocing Wang, Yu Lu, Qiang Li, Xunqiang Tao, Yandong Guo, Mingming Gong, and Tongliang Liu. 2022. CRIS: CLIP-Driven Referring Image Segmentation. In *IEEE Conference on Computer Vision and Pattern Recognition (CVPR)*. 11686–11695.

[50] Ziyu Wei, Xi Yang, Nannan Wang, and Xinbo Gao. 2022. RBDF: Reciprocal bidirectional framework for visible infrared person reidentification. *IEEE Transactions on Cybernetics* 52, 10 (2022). 10988–10998.

[51] Ziyu Wei, Xi Yang, Nannan Wang, and Xinbo Gao. 2024. Dual-Adversarial Representation Disentanglement for Visible Infrared Person Re-Identification. *IEEE Transactions on Information Forensics and Security* 19 (2024). 2186–2200.

[52] Ancong Wu, Wei-Shi Zheng, Hong-Xing Yu, Shaogang Gong, and Jianhuang Lai. 2017. RGB-Infrared Cross-Modality Person Re-identification. In *IEEE International Conference on Computer Vision (ICCV)*. 5390–5399.

[53] Jianbing Wu, Hong Liu, Yuxin Su, Wei Shi, and Hao Tang. 2023. Learning Concordant Attention via Target-aware Alignment for Visible-Infrared Person Re-identification. In *IEEE International Conference on Computer Vision (ICCV)*. 11122–11131.

[54] Qiong Wu, Pingyang Dai, Jie Chen, Chia-Wen Lin, Yongjian Wu, Feiyue Huang, Bineng Zhong, and Rongrong Ji. 2021. Discover cross-modality nuances for visible-infrared person re-identification. In *IEEE Conference on Computer Vision and Pattern Recognition (CVPR)*. 4330–4339.

[55] Qiong Wu, Jiaer Xia, Pingyang Dai, Yiyi Zhou, Yongjian Wu, and Rongrong Ji. 2025. CycleTrans: Learning Neutral Yet Discriminative Features via Cycle Construction for Visible-Infrared Person Re-Identification. *IEEE Transactions on Neural Networks and Learning Systems* 36, 3 (2025). 5469–5479.

[56] Shuanglin Yan, Neng Dong, Shuang Li, and Huafeng Li. 2025. TriMatch: Triple Matching for Text-to-Image Person Re-Identification. *IEEE Signal Processing Letters* 32 (2025). 806–810.

[57] Shuanglin Yan, Neng Dong, Jun Liu, Liyan Zhang, and Jinhui Tang. 2023. Learning Comprehensive Representations with Richer Self for Text-to-Image Person Re-Identification. In *ACM International Conference on Multimedia (ACM MM)*. 6202–6211.

[58] Shuanglin Yan, Neng Dong, Liyan Zhang, and Jinhui Tang. 2023. CLIP-Driven Fine-grained Text-Image Person Re-identification. *IEEE Transactions on Image Processing* 32 (2023). 6032–6046.

[59] Shuanglin Yan, Jun Liu, Neng Dong, Liyan Zhang, and Jinhui Tang. 2024. Prototypical Prompting for Text-to-image Person Re-identification. In *ACM International Conference on Multimedia (ACM MM)*. 2331–2340.

[60] Shuanglin Yan, Hao Tang, Liyan Zhang, and Jinhui Tang. 2024. Image-Specific Information Suppression and Implicit Local Alignment for Text-Based Person Search. *IEEE Transactions on Neural Networks and Learning Systems* 35, 12 (2024). 17973–17986.

[61] Shuanglin Yan, Yafei Zhang, Minghong Xie, Dacheng Zhang, and Zhengtao Yu. 2022. Cross-domain person re-identification with pose-invariant feature decomposition and hypergraph structure alignment. *Neurocomputing* 467 (2022). 229–241.

[62] Mouxing Yang, Zhenyu Huang, Peng Hu, Taihao Li, Jiancheng Lv, and Xi Peng. 2022. Learning With Twin Noisy Labels for Visible-Infrared Person Re-Identification. In *IEEE Conference on Computer Vision and Pattern Recognition (CVPR)*. 14308–14317.

[63] Lewei Yao, Runhui Huang, Lu Hou, Guansong Lu, Minzhe Niu, Hang Xu, Xiaodan Liang, Zhenguo Li, Xin Jiang, and Chunjing Xu. 2022. FILIP: Fine-grained Interactive Language-Image Pre-Training. In *International Conference on Learning Representations (ICLR)*.

[64] Mang Ye, Jianbing Shen, Gaojie Lin, Tao Xiang, Ling Shao, and Steven C. H. Hoi. 2022. Deep Learning for Person Re-Identification: A Survey and Outlook. *IEEE Transactions on Pattern Analysis and Machine Intelligence* 44, 6 (2022). 2872–2893.

[65] Mang Ye, Zesen Wu, Cuiqun Chen, and Bo Du. 2024. Channel Augmentation for Visible-Infrared Re-Identification. *IEEE Transactions on Pattern Analysis and Machine Intelligence* 46, 4 (2024). 2299–2315.

[66] Xiaoyan Yu, Neng Dong, Liehuang Zhu, Hao Peng, and Dapeng Tao. 2025. CLIP-Driven Semantic Discovery Network for Visible-Infrared Person Re-Identification. *IEEE Transactions on Multimedia* (2025). 1–13. <https://doi.org/10.1109/TMM.2025.3535353>

[67] Guiwei Zhang, Yongfei Zhang, and Zichang Tan. 2023. ProtoHPE: Prototype-guided High-frequency Patch Enhancement for Visible-Infrared Person Re-identification. In *ACM International Conference on Multimedia (ACM MM)*. 944–954.

[68] Liyan Zhang, Guodong Du, Fan Liu, Huawei Tu, and Xiangbo Shu. 2021. Global-Local Multiple Granularity Learning for Cross-Modality Visible-Infrared Person Reidentification. *IEEE Transactions on Neural Networks and Learning Systems* (2021). 1–11.

[69] Qiang Zhang, Changzhou Lai, Jianan Liu, Nianchang Huang, and Jungong Han. 2022. Fmcnet: Feature-level modality compensation for visible-infrared person re-identification. In *IEEE Conference on Computer Vision and Pattern Recognition (CVPR)*. 7349–7358.

[70] Yafei Zhang, Yongzeng Wang, Huafeng Li, and Shuang Li. 2022. Cross-compatible embedding and semantic consistent feature construction for sketch re-identification. In *ACM International Conference on Multimedia (ACM MM)*. 3347–3355.

[71] Yukang Zhang, Yan Yan, Yang Lu, and Hanzi Wang. 2021. Towards a Unified Middle Modality Learning for Visible-Infrared Person Re-Identification. In *ACM International Conference on Multimedia (ACM MM)*. 788–796.

[72] Xian Zhong, Tianyou Lu, Wenxin Huang, Mang Ye, Xuemei Jia, and Chia-Wen Lin. 2021. Grayscale enhancement colorization network for visible-infrared person re-identification. *IEEE Transactions on Circuits and Systems for Video Technology* 32, 3 (2021). 1418–1430.

[73] Kaiyang Zhou, Jingkang Yang, Chen Change Loy, and Ziwei Liu. 2022. Learning to prompt for vision-language models. *International Journal of Computer Vision* 130, 9 (2022). 2337–2348.